2015 IEEE/RSJ International Conference on Intelligent Robots and Systems (IROS)
Congress Center Hamburg
Sept 28 - Oct 2, 2015. Hamburg, Germany

Development of a Lower Extremity Exoskeleton Robot with a Quasi-anthropomorphic Design Approach for Load Carriage

Donghwan Lim[1], Wansoo Kim[1], Heedon Lee[1], Hojun Kim[1],
Kyoosik Shin[2], Taejoon Park[2], JiYeong Lee[2], and Changsoo Han[2*]

Abstract— **This study developed the Hanyang Exoskeleton Assistive Robot (HEXAR)-CR50 aimed at improving muscle strength of the wearer while transporting a load. The developed exoskeleton robot HEXAR-CR50 has 7 degrees of freedom (DOF) for one foot, 3-DOF for the hip joints, 1-DOF for the knee joints, and 3-DOF for the ankle joints. Through functional analysis of each human joint, two DOFs were composed of active joints using an electric motor developed in an under-actuated form with heightened efficiency. The rest of the DOFs were composed of passive or quasi-passive joints to imitate human joints. The control of the exoskeleton robot was based on the physical human-robot interaction. In order to verify the performance of the developed HEXAR-CR50, muscle activity was measured using electromyography, vGRF was measured using F-Scan sensor. The experimental results showed that %MVIC was reduced against the external load applied, while GRF had a decrement rate, compared with the external load when the exoskeleton was worn, which verified the performance in accordance with the development objective of load carrying. A muscle strength augment effect from the developed wearable robot was verified.**

I. INTRODUCTION

An exoskeleton robot system is a mechanical structure that is attached to the exterior of a human body to improve the muscular power of the wearer. Exoskeleton robots have been actively studied in the US, Japan, and Europe since the 1990s , and research is currently being conducted to identify their application in various industries, including the military, medicine, and rehabilitation. The exoskeleton is divided into either a power assistance or a power augmentation system, depending on its purpose. And, depending on its design structure of the alignment to the rotation axis of the robot joint and the rotation axis of the human joint, the exoskeleton may be classified as anthropomorphic, quasi-anthropomorphic, or non-anthropomorphic [1].

The power assistance system adds power to the wearer's external skeleton because it supports the human body via the exoskeleton. The MIT, HAL, ALEX, and HARO exoskeleton systems have been developed as supplementary support for the elderly and disabled persons to enable normal daily living. As mentioned, these exoskeletons are designed anthropomorphically. In addition, the EKSO exoskeleton systems is designed quasi-anthropomorphically[2]-[6]. On the other hand, the power augmentation system amplifies the power of the wearer through the exoskeleton, thereby enabling high-load carrying motions, which would otherwise be difficult. The BLEEX, HULC, and XOS exoskeleton systems were developed with the aim for use in industrial and military campaign environments, where heavy loads are carried or manipulated. These exoskeletons are designed quasi-anthropomorphically. In addition, the WAD exoskeleton systems was designed non-anthropomorphically[7]-[10].

In this study, we propose a lower exoskeleton system designed to carry a heavy load. We analyzed the human joint function to design the joint modules of the exoskeleton robot. We designed an exoskeleton robot through a quasi-anthropomorphic architecture. This paper focuses on the setup of the mechanical structure and the design of the HEXAR-CR50 through the functions of each joint. In addition, we confirm the effectiveness of the exoskeleton robot through experiments.

II. MECHANICAL DESIGN OF EXOSKELETON ROBOT

A. Structure of Exoskeleton Robot

The exoskeleton structure is placed on the human wearer, and it generates a moment according to the payload. In order for the generated moment not to affect the wearer, it is necessary to maintain a constant rigid state in the stance phase. To maintain a constant rigid state, some robot joints should be misaligned with the human joints, thereby delivering payloads to the ground. Thus, a quasi-anthropomorphic architecture was selected for efficiency and human motion synchronized controllability to achieve the load carrying goal of the HEXAR-CR50. Fig. 1 shows the arrangement of the DOF selected for each joint and joint type. We developed an under-actuated exoskeleton consisting of 7 degrees of freedom(DOF) per leg. Based on the gait power analysis, the hip and knee extension/flexion joints were selected to be active. And Ankle dorsiflexion/plantarflexion joints were selected to be quasi-passive mechanisms.

The remaining joints were selected to be passive with mechanical limitations because range of motion(ROM), moment, and power were low.

The HEXAR-CR50 is of an under-actuated type and applies a quasi-anthropomorphic mechanism in which some of the robot's DOFs are different from human DOFs in order to achieve the goal of load carrying. In addition, the goal weight of the design was 23 kg, and the system was designed to carry a payload of 20-30kg. Before designing a joint or actuator, information on the desired range of motion for each joint is needed. To avoid potential harm to the operator, the range of motion in the exoskeleton joint should be limited

[1]Department of Mechanical Engineering, Hanyang University, Seoul, South Korea blackfire857@gmail.com
[2*]Department of Robot Engineering, Hanayng University ERICA, Ansan, South Korea cshan@hanyang.ac.kr

Fig. 1: Exoskeleton structure design and Joint Modules

to less than that of human flexibility. Table I shows a ROM which is set to the design of the HEXAR-CR50.

TABLE I: Ranges of motion for the joints of HEXAR-CR50

	Joint axis	Angle(deg)	
		Min.	Max.
Hip	Internal/external rotation	-10	10
	Extension/flexion	-40	150
	Adduction/Abduction	-7	35
Knee	Extension/flexion	0	127
Ankle	Internal/external rotation	-10	10
	Plantarflexion/dorsiflexion	-30	30
	Eversion/inversion rotation	-10	10

B. Design of Joint Modules

1) Active Joint Module: Several assumptions were made in order to select and size the actuator. The first assumption was that the size, mass, and inertial properties of the exoskeleton were equivalent to those of a human. The second was that the human and exoskeleton joints move along the same axis. The third was that the maximum external loads permitted were 30 kg.

The joint speed required for hip joints was a maximum of 4.6 rad/sec, and -2Nm/BW of torque was required for level walking at 6 km/h with 30kg. The joint speed required for knee joints in the same environment was a maximum of 7 rad/sec. However, most motions are done within 4 rad/sec, and motions faster than 5 rad/sec are done momentarily.

The active joint module refers to a module consisting of an electrical motor and harmonic gear. It is applied to the hip and knee extension/flexion joint. The selected motors are pancake-shaped, and a component-type harmonic drive was selected in order to minimize the weight and width of the joint module. The BLDC's motor specifications can be selected according to the characteristics of current and torque. The motor produces the following torque, which is proportional to the motor current i, such that $\tau = k_t \cdot i$, where k_t is the motor torque constant. For the steady-state

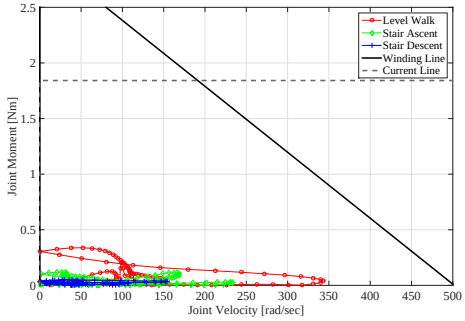

(a) Hip joint velocity vs. moment

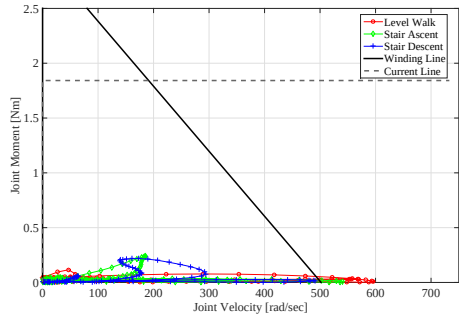

(b) Knee joint velocity vs. moment

Fig. 2: The required motor torque for the hip and knee as calculated from the gait analysis data for walking

torque-speed relationship, the voltages around the loop are summed and rearranged for i by the following equation:

$$i = \frac{V - v_b}{R} = \frac{V - k_v \omega}{R} \tag{1}$$

where v_b is the motor back-EMF in the armature, V is the voltage applied to the motor, k_v is the back-EMF constant, R is the motor's resistance, and ω is the angular velocity. Substitute this value of i into the following equation for the maximum theoretical torque:

$$\tau_{max} = \frac{k_t}{R}\left(V_{max} - k_v \omega\right) \tag{2}$$

Therefore, the required torque must be less than τ_{max} from the motor winding [7]. The final limit of the motor's capabilities is the current limit; I_p is based on the maximum current density in the winding and is available for a maximum duration of 10 seconds. If the lowest of these is I_p and the maximum torque τ_p, the winding can produce the torque at any motor speed. It is calculated as follows :

$$\tau_p = k_t I_p \tag{3}$$

The required joint torque τ_{req} and speed ω_{req} are translated to the absolute values. With a harmonic drive gear ratio of N, the required motor torque T and ω are calculated by

$$T = \frac{T_{req}}{N} \tag{4}$$

$$\omega = \omega_{req} N \tag{5}$$

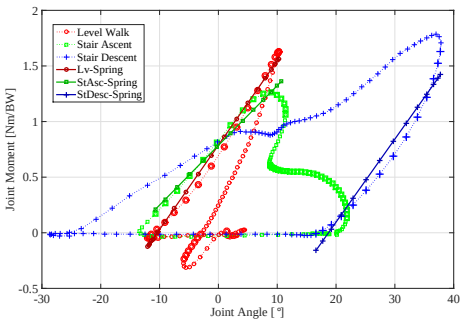

Fig. 3: Ankle dorsiflexion/plantar flexion motion analyses for selecting the spring constant k_h during level walking, stair ascent, and stair descent

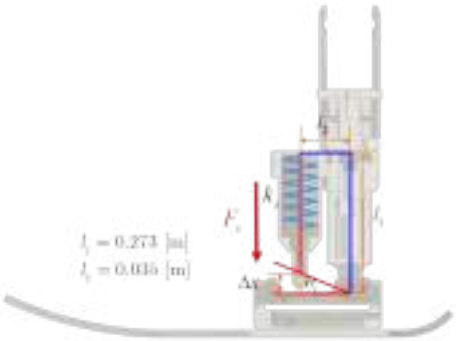

Fig. 4: Design of the quasi-passive mechanism for the ankle dorsiflexion/plantarflexion joint

Fig.2 shows that the required motor torque-speed characteristics for the HEXAR-CR50's joints were calculated and plotted for various walking environments. Stair ascent and descent, with the winding torque line, were lower than the current torque line. However, the required torque-velocity curve of level walking for the knee joint exceeded the short-term operation limit of the actuator in the transition from extension to flexion. In order to satisfy the required torque, only upgrading of the motor should be needed.

However, this research did not consider this aspect because of the short timeframe available for actuating the motion. The parameters of the electrical motors that were selected to power the flexion joints of the HEXAR-CR50 are shown in Table II.

2) Quasi-passive Joint Module: Ankle dorsiflexion/plantarflexion joint absorbs energy during the first half of the stance phase and releases energy just before toe-off. Power is generated by the moment and joint velocity, whereas the ankle joint moment is not generated significantly. That is, changes in the joint moment are small, but large joint velocity is required. Furthermore, the region where ankle power is applied is about 10% of the gait cycle, which is inefficient since instant power is generated to control the active joints. To satisfy this function, quasi-passive mechanisms were designed with compliance material to support the weight of external loads in the stance phase and to absorb or release the energy.

TABLE II: Electric motor and harmonic gear selected for HEXAR-CR50

Parts	Parameters	Value	Unit
Motor	Motor torque constant, k_t	0.061	Nm/A
	Input voltage, V	29.4	V
	Nominal speed	4601	RPM
	Nominal torque	0.429	Nm
	Nominal current	7.39	A
	Back-EMF constant, v_b	6.39	V/kRPM
	Motor resistance, R	0.615	Ω
	Current limit, I_p	30.2	A
Harmonic gear	Transmission ratio, N	100	-
	Continuous torque	34	Nm
	Stall torque	57	Nm
	Efficiency	90	%

The joint used for dorsiflexion and plantarflexion demands a large moment during the gait. Power absorption and generation occur repetitively, according to the gait phase[13]. Fig.3 shows the results of the gait analysis for the angle-moment relationship during level walking and stair climbing.

The stance phase may be divided into the dorsiflexion section, where power absorption takes place, and the plantarflexion section, where power generation occurs. This study proposes a mechanism in which the power stored during the dorsiflexion motion by using a spring is used during plantarflexion. The approximate spring constant can be known from the relationship between angle and moment in the results of the gait analysis. When the body weight of the exoskeleton is 23 kg, the mean value of the spring constant k_h is about 0.068 Nm/BW·deg with three different walking conditions. The quasi-passive module refers to a passive joint that can generate a force by applying spring elements; it is applied to the dorsi-plantarflexion motion of the ankle joint. The spring constant k_h to generate the ankle propulsion torque is analyzed in Table III.

The spring constant (k_s) of the spring used for this mechanism may be calculated using (6). Here, τ_h is the conversion of the results of the gait analysis to the body weight of the exoskeleton. It can be expressed as $\tau_h = k_h \cdot \theta_r$. Consequently, the spring constant was determined to be $69.6 N/mm$. Fig.4 shows the design of an ankle mechanism for the dorsiflexion and plantarflexion motions.

$$k_s = \frac{k_h \theta_r}{\Delta x_l l_2} \tag{6}$$

$$where, \quad \Delta x_s = l_2 \tan\theta_r \ (0^\circ \le \theta_r \le 30^\circ)$$

$$\tau_h = \tau_S, k_h \theta_r = k_s \Delta x_s l_2$$

III. Exoskeleton Robot Controller

A. Controller Architecture

The control law relies on the real-time model of the system, and kinematic and dynamic data must be continuously monitored. Kinematic variables require joint angles,

TABLE III: Ankle spring constant k_h for the plantarflexion motion while walking

Spring constant (Nm/BW·deg)			Mean
Level walking	Stair ascent	Stair descent	
0.0758	0.0537	0.0747	0.068

velocities, and angular acceleration that can be measured and estimated by the rotary encoders. The absolute foot angle is also needed to measure the orientation of the upper body with respect to gravity, using an attitude heading reference system (AHRS). To select the gait control at each phase, an insole sensor was developed as well as to detect the gait phase through the center of pressure (COP). In the stance phase control, to measure the human-robot interaction force, a multi axis force/torque sensor was mounted in the harness module between the human and robot. Finally, the torque applied by the actuator was measured by the torque sensor, and it is used for both joint force feedback control and human-robot interaction force estimation. The controller structure is composed of a main controller, a sensor control unit (SCU), and a motor control unit (MCU). To implement the control algorithm, the main controller communicates with the other control units to obtain the sensor signal and send the command. The SCU is responsible for acquiring the sensor signal and transmitting it to the main controller by converting it to a communication signal. The MCU performs the joint feedback control and sends commands to the actuator.

B. Control Law with Human-Robot Interaction Force

As discussed in the previous section, each leg has two actuated DOF: the hip and knee joints in the sagittal plane. In order for the leg to walk with a human motion, we consider two distinct gait phases and select two different control models. Fig.5 shows the block diagram of the control law for the exoskeleton leg. The human-robot interaction force, T_{int}, affects the exoskeleton by distinguishing the position with impedance, k_h. The main tracking objective of this control law that was T_{int} going to zero. The gait phase could be detected by the insole sensors and by switching the control laws for the stance or swing phase. In the stance phase, the control law uses a sensor that measures the human-robot interaction force, $F_{intST} = [F_x F_y F_z]^T$, at the harness module. The joint torques caused by the human, $T^{'}_{intST}$, are computed in (7).

$$\vec{T}^{'}_{intST} = J^T \vec{F}_{intST} \tag{7}$$

In swing, the inertial reference frame can be arbitrarily selected to be the harness module. The estimate of the T_{intSW} through the virtual control law is thus as follows (8).

$$\vec{T}^{'}_{intSW} = B(q)\,\ddot{q} + C(q,\dot{q})\,\dot{q} + G(q) - \vec{T}_a \tag{8}$$

These joint torques can now be used in the force control scheme, and they can added to the gravity compensation

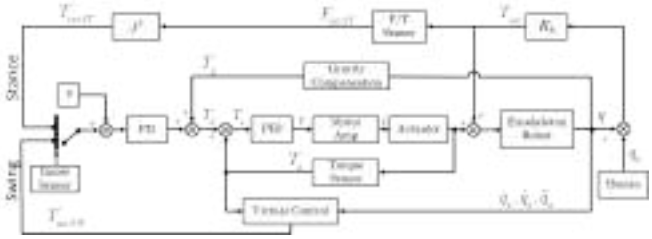

Fig. 5: HRI Based Control law for the Exoskeleton Leg.

torque, T_g. These desired torque, T_d, was used in joint torque feedback control with actual torque, T_a.

IV. Experiment and Discussion

The exoskeleton HEXAR-CR50 developed in this study was designed to achieve power augmentation by reducing the load bearing on the human body during load-carrying motions. That means to develop a exoskeleton system that can assist individuals who must carry loads for extended period time. During human walking, a substantial amount of power consumption can measure by the metabolic power rate. Many researchers have attempted to reduce the metabolic burden on load carriage by developing exoskeletons [11], [12]. To verify the metabolic power effect, the forces generated by the human or the forces directly applied to the human to achieve motions were measured and analyzed. However, the data that can be measured through human are extremely limited. Among them, EMG sensors are generally used to measure muscle activity during movement. They are also used to represent muscle usage [13]. If muscle activity during movement is measured using EMG, it can be utilized in the verification of the exoskeleton effect because it can demonstrate muscle usage. In addition, the forces applied to external load objects are transmitted to the ground through the human body so that the forces caused by the load can be analyzed by measuring the vGRF between the human and the ground. Force sensors of the insole type can be used to measure vGRF. The effect on the exoskeleton can be observed separately because the sensors are located between the human and the shoes while the forces are measured. Thus,

Fig. 6: Experimental setup of the power augmentation effect in level walking.

two sensors were used to verify the metabolic power effect on load carrying by the exoskeleton.

A. Experimental Setup

The experiment was conducted in one subject (age: 29, weight: 75 kg). One subject was healthy and had no gait impairment. The EMG sensor used is a four-channel surface EMG (LAXTHA). The sensor used for the vGRF measurement was F-Scan in the shoe sensor of EMG. The performance of the robot was verified through the gait experiments using the above two sensors. The experimental results indicate the exoskeleton wearing and one without exoskeleton wearing by measuring sensor signals and compared with two experiment results. The experimental conditions were external load conditions were 10, and 20 kg while walking on level ground at a constant speed (3 km/h). All experiments repeated five sets in which the external load condition was changed sequentially. The experimental conditions and procedures are shown in Fig. 6.

EMG electrodes were attached to the four main muscles used while walking: vastus lateralis and medialis, gastrocnemius, and soleus. The sampling frequency of the EMG sensor measurement and F-scan sensor with Tekscan devices were at 512 Hz. The frequencies of two devices were matched through a trigger because they were measured by their own software. To express EMG sensor signals as quantitative muscle strength, the normalized technique, percent maximum voluntary isometric contraction (%MVIC) was used. Equation(9) shows the calculation of %MVIC [14].

$$\%MVIC = \frac{RMS_{muscle}}{MVIC} \tag{9}$$

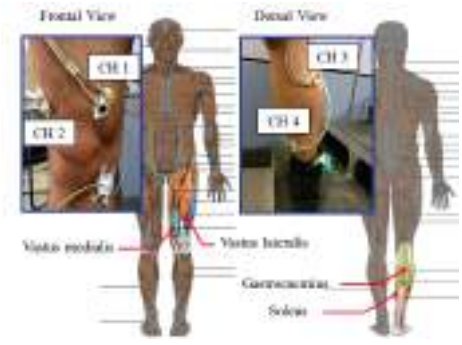

(a) Attachment positions of the EMG electrodes in the muscle

(b) Attachment positions of the F-scan sensor between the human foot and foot module

Fig. 7: Sensors positions of EMG and F-scan sensor

where RMS_{muscle} is the root mean square (RMS) value of the measured signal, and %MVIC is the maximum muscle strength. %MVIC is represented for each muscle, so %MVIC was measured accordingly. The method of measurement differed according to the locations of the muscles. Because the maximum muscle was measured, the measurement was conducted immediately after the electrodes were attached and re-measured when the electrodes were changed. Fig.7(a) shows the sensor settings in the experiment, the muscles attached to electrodes, and the %MVIC measurement method. Fig.7(b) shows the F-scan sensor position setting for measure the vGRF between the human and ground.

B. Experimental Result

Fig.8(a) shows the %MVIC of comparing the EMGs measuring with or without wearing the exoskeleton. When the exoskeleton was worn and the external load applied, most %MVIC values were lower than when the exoskeleton was not worn. In particular, %MVIC values increased linearly when the exoskeleton was not worn yet were constant when the exoskeleton was worn. In the case of the soleus muscle, %MVIC decreased when the exoskeleton was worn compared to when it was not worn. This verified that the ankle joint module, the quasi-passive joints developed in this study, had normal function. The experimental data result of the %MVIC while not wearing and wearing the exoskeleton are summarized in Table IV.

Fig.8(b) shows the vGRF of comparing the TEKSCAN measuring with or without wearing the exoskeleton. Mea-

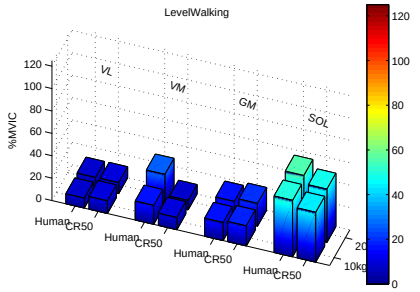

(a) The %MVIC during level walking

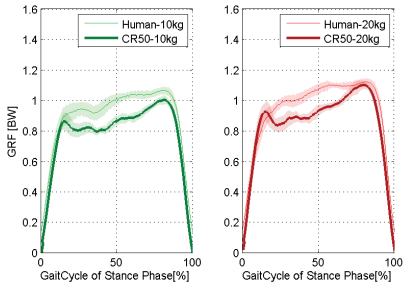

(b) The vGRF during level walking

Fig. 8: Comparison of the experimental result of the %MVIC and vGRF while not wearing and wearing the exoskeleton

TABLE IV: Experimental data result of the %MVIC while not wearing and wearing the exoskeleton

Experiment conditions		Human without Exoskeleton %MVIC (%)			
		VL*	VM†	GM‡	SOL§
Level walking	10kg	8.97	17.00	16.19	50.53
	20kg	9.74	27.08	17.39	55.08

Experiment conditions		Human with Exoskeleton %MVIC (%)			
		VL*	VM†	GM‡	SOL§
Level walking	10kg	11.38	10.95	18.04	44.70
	20kg	9.89	8.46	20.40	47.60

* Vastus lateralis muscle
† Vastus medialis muscle
‡ Gastrocmemius medialis muscle
§ Soleus muscle

TABLE V: Decrement rate of vGRF impulse for stance phase under the experiment conditions

Experiment conditions		vGRF impulse ($\times 10^3$)		Decrement rate (%)
		Without Exo	With Exo	
Level walking	10kg	3.93	3.59	9.46
	20kg	4.25	3.95	7.67

sured vGFR values were represented by the gait cycle of the stance phase. The measured vGRF data can be analyzed through the gait phase from the initial contact of 0% to the toe-off of 100%. The experimental results were expressed as mean (SD) with respect to the repeated experiments.Compared to the experimental result, the application of the worn the exoskeleton condition significantly affects vGRF parameters. The first vGRF peak value is much higher, the second vGRF peak value is lower. The increase in the early vGRF peak value therefore suggests that the exoskeleton did not absorb the impact of the heel strike. This might be because the ankle quasi-passive joint was acting on the plantar flexion only. vGRFs were lower when the exoskeleton was worn while at 30∼70% stance phase. This fact relates to external loads not acting on the human, but which transmitted to the ground through the exoskeleton. That results of the decrement rate indicates to the impulse for 30∼70% of gait phase, as shown in Table V.

V. CONCLUSIONS

Through this study, a lower-extremity exoskeleton, called HEXAR-CR50, was developed for industry and military purposes, particularly to achieve power augmentation during load carrying. To develop the exoskeleton, the design specifications of the system were based on biomechanical considerations and gait analysis. The design goal was a system within a 23 kg weight, and the specification was selected accordingly. Based on the design specification, an exoskeleton of a semi-anthropomorphic architecture was designed, and joint shapes and layouts were studied. In the design, each leg had 7-DOF and was configured with a combination of active and passive joints. An electrical motor and harmonic gears were applied to the extension and flexion joints of hips and knees, and springs were applied to the ankle and toe joints, which resulted in a quasi-passive mechanism. The experimental results showed that %MVIC was reduced against the external load applied, while vGRF had a decrement rate, compared with the external load when the exoskeleton was worn, which verified the performance in accordance with the development objective of load carrying. In the future, simplified control algorithms, a lightweight mechanical structure, and miniaturization will be used to improve the efficiency of the current exoskeleton.

ACKNOWLEDGMENT

This work was supported by the Duel-Use Technology Program of MOTIE/DAPA/CMTC.[13-DU-MC-16], and the National Research Foundation of Korea(NRF) grant funded by the Korea government(MEST).(No.NRF-2015R1A2A2A01002887)

REFERENCES

[1] Heedon Lee, Wansoo Kim, Jungsoo Han, and Changsoo Han. The technical trend of the exoskeleton robot system for human power assistance, International Journal of Precision Engineering and Manufacturing, 13(8) pp.1491-1497, 2012.
[2] C.J. Walsh, K.Endo, H. Herr, A qusi-passive leg exoskeleton for load-carrying augmentation, International Journal Humanoid Robotics, 4, pp.487-506, 2007.
[3] CYBERDYNE Inc., Robot Suit HAL, http://www.cyberdyne.jp/english/index.html
[4] Sai K. Banala, Seok Hun Kim, Sunil K. Agrawal, John P. Scholz, Robot Assisted Gait Training With Active Leg Exoskeleton(ALEX), IEEE/RAS-EMBS International Conference on Biomedical Robotics and Biomechatronics, pp.19-22, 2008.
[5] Morichita. S., Tanaka. T., Yamafuji. K., Knamori. N.,Improvement of Maneuverability of the Man-Machine System for Wearable Nursing Robots, Journal of Robotics and Mechatronics, Vol.11, N0.6, pp.461-467, 1999.
[6] K. A. Strausser, H. Kazerooni, The Development and Testing of a Human Machine Interface for a Mobile Medical Exoskeleton, 2011 IEEE/RSJ International Conference on Intelligent Robots and Systems, pp. 4911-4916, 2011.
[7] A. Zoss, H. Kazerooni and A. Chu, On the mechanical design of the Berkeley Lower Extremity Exoskeleton (BLEEX), IEEE/RSJ International Conference on Intelligent Robots and Systems, pp.3132-3139, 2005.
[8] R. Bogue, Exoskeleton and robotic prosthetics: a review of recent developments, Industrial Robot, Vol. 36, no.5, pp.421-427, 2009.
[9] S.C. Jacobsen, On the development of XOS, a powerful exoskeletal robot, IEEE/RSJ International Conference on Intellingent Robots and Systems, 2007.
[10] Y. Ikeuchi, J. Ashihara, Y. Hiki, H. Kudoh and T. Noda, Walking assist device with bodyweight support system,, IEEE/RSJ International Conference on Intelligent Robots and Systems, pp. 4073-4079, 2009.
[11] Gregory S Sawicki, Daniel P Ferris, Powered ankle exoskeletons reveal the metabolic cost of plantar flexor mechanical work during walking with longer steps at constant step frequency, Journal of Experimental Biology, pp.21-31, 2009.
[12] Luke M Mooney, Elliott J Rouse, Hugh M Herr., Autonomous exoskeleton reduces metabolic cost of human walking during load carriage, Journal of NeuroEngineering and Rehabilitation, 2014.
[13] W.S. KIM, H.D. LEE, D.H. LIM and C.S. HAN, Development of a Lower Extremity Exoskeleton System for Walking Assistance while Load Carrying, International Conference on Climbing and Walking Robots, pp.35-42, 2013.
[14] M.Nordin and V.H. Frankel, Basic Biomechanics of the Musculoskeletal System, 3rd end. Lippincott Williams and Wilkins, Baltimore, MD, 2001.